09;07.3

Heating of a quantum cascade laser under pulsed pumping: theory and experiment

© I.I. Vrubel[1], E.D. Cherotchenko[1], D.A. Mikhailov[1], I.I. Novikov[2], D.S. Papylev[2], D.V. Chistyakov[1], N.G. Deryagin[1], V.Yu. Mylnikov[1], S.H. Abdulrazak[1], V.V. Dudelev[1], G.S. Sokolovskii[1]

[1] Ioffe Institute, St. Petersburg, Russia
[2] ITMO University, St. Petersburg, Russia
E-mail: echerotchenko@gmail.com

Received November 20, 2023
Revised December 13, 2023
Accepted December 13, 2023

The paper considers the features of the quantum cascade laser operation under pulsed current pumping and corresponding heating. We have shown that, as the steepness of the pump pulse front edge decreases, the threshold current shifts towards higher values by tens of milliamps, which is associated with intense heating of the QCL active region in the first moments after the start of pumping. A model based on the thermodiffusion approximation is proposed to describe the experiment. Studying the time dependence of laser radiation intensity has shown that, within the interval of hundreds of nanoseconds after the pump pulse onset, power transfer to the main heat sink gets activated; thereat, the heat removal efficiency reaches 50−75% of the total power consumption, which significantly reduces the rate of active region heating.

Keywords: integrated optics, quantum cascade laser.

DOI: 10.61011/PJTF.2024.07.57460.19807

Quantum cascade lasers (QCLs) are unipolar semiconductor devices emitting in the mid— and far-infrared ranges. The idea proposed in 1971 [1] and experimentally implemented for the first time in 1994 [2] is today a universal platform for solving many applied problems in various fields, such as biomedicine [3], security system components [4], environmental monitoring [5], and also wireless optical communications [6]. Such a wide range of applications is associated with unique properties of the mid-infrared range containing intense absorption lines of various molecules, as well as two windows of atmospheric transparency. At present, one of the main tasks in developing the QCL technology is to increase their efficiency, which, however, is a non-trivial task [7]. Despite the fact that the quantum cascade laser efficiency reaches tens of percent [8], the energy released during operation in the form of heat affects the basic QCL parameters even in the case of operation in the pulsed pump mode. Excessive heating of the laser active region induces variations in threshold characteristics and degradation of laser radiation. Hence, possible overheating of the active region worsens the laser functional characteristics, makes more difficult implementation of the continuous lasing mode, and requires careful consideration of the impact of external conditions on the QCL functioning. In this work, we study the dynamics of heating the QCL active region under sub-microsecond pulsed pumping.

In the experiments, QCL samples similar to those used in [9–11] were employed. Based on the radiation power peak, QCL watt-ampere characteristics were constructed, whose variable parameter was the time constant of the pump pulse front edge. The watt-ampere characteristics were measured in the QCL pulsed operating mode with the pulse repetition rate of 11.5 kHz and pump pulse width of 500 ns. Mean power was measured by using a Thorlabs PM100 power meter with calibrated thermoelectric sensor S401C. The radiation dynamic characteristics were studied with the aid of a thermoelectrically cooled photodetector Vigo Systems PVI-4TE-10.6 having the bandwidth of 1ĠHz, which operated in the reverse bias mode. For the analysis, a pumping mode with the current amplitude of 4.5Å was chosen. The measurement technique is also described in [12]. The current pulses shown in Fig. 1, *a* are characterized by different front edge steepnesses which were adjusted by tuning the QCL pumping electrical circuit so as to increase the circuit active resistance without changing the reactance. An increase in the delay between the current pulse onset and reaching the threshold results in that the power released in the form of heat warms up the active region bulk, which causes the active region overheating by a few degrees relative to the starting conditions and reduces instantaneous peak power of the optical signal ($A_{\max}$). This, in turn, leads to a shift in threshold current I_{thr} by a few percent (tens of milliamps) in measuring the watt-ampere characteristic (Fig. 1, *b*):

$$I_{thr}(T) = I_{thr} \exp\left(\frac{T}{T_0}\right) \approx I_{thr}\left(1 + \frac{T(t)}{T_0}\right). \qquad (1)$$

Detailed information on the dynamics of heating the active region can be obtained by analyzing the radiation pulse time sweep. Fig. 2, *a* schematically illustrates a model

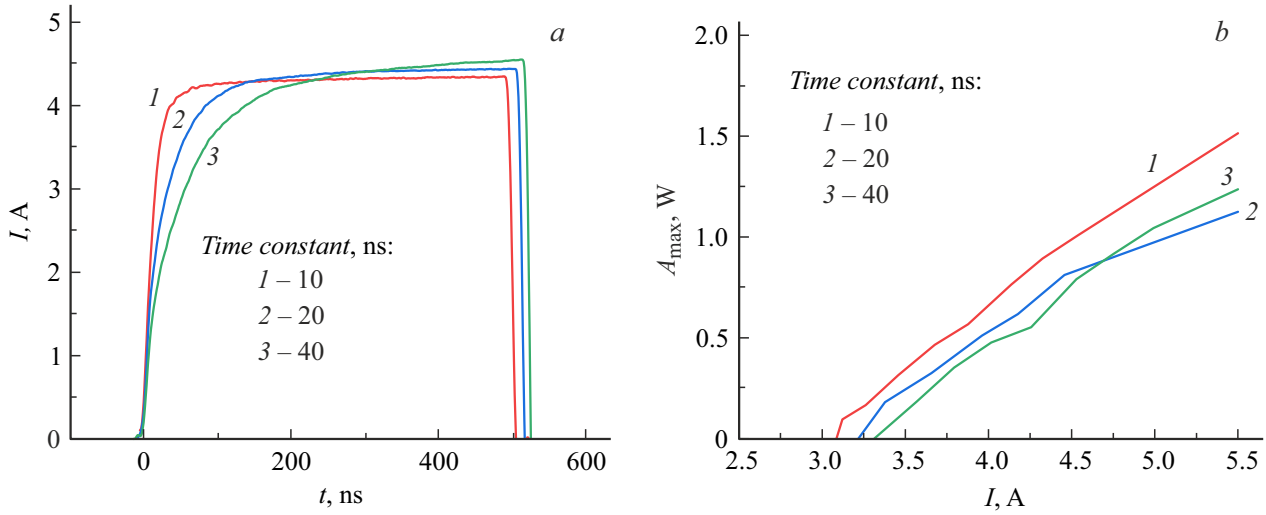

Figure 1. *a* —time dependence of the pump current strength of the generator with the tunable time constant of 10, 20 and 40 ns at one and the same equilibrium amplitude of 4.5 A. *b* — watt-ampere characteristic of the QCL sample measured based on the peak radiation intensity value (A_{max}) for pump pulses shown in panel *a*.

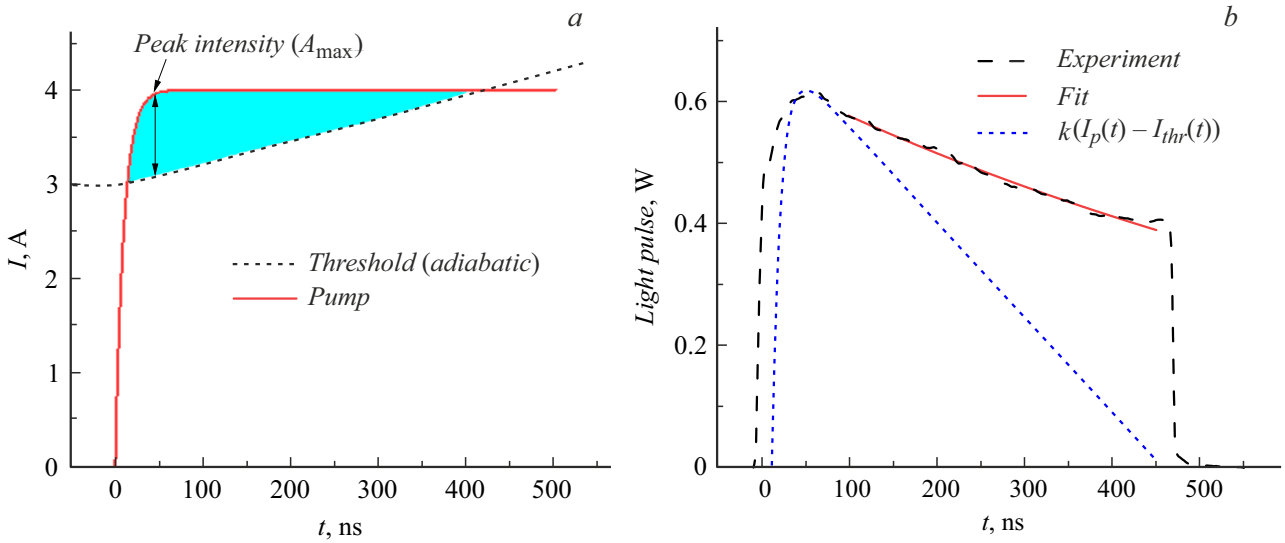

Figure 2. *a* — model time sweep of the pump pulse current approximating experimental measurements (solid line), and threshold currents calculated in the adiabatic heat-release approximation (dashed line). The time interval in which the pump current exceeds the threshold value (shaded area) corresponds to the presence of radiation. The arrow indicates pumping at the time point corresponding to maximum peak intensity A_{max}. *b* — experimentally measured radiation pulse time sweep at pump current of 4.5 A (dashed line) and its exponential approximation (solid line) in the region far from transient processes. The dotted line represents a theoretical estimate of the radiation intensity obtained under the assumption that the pump pulse front edge is exponentially shaped and power release mode is adiabatic.

description of processes taking place in QCL under pulsed pumping. The solid curve symbolically represents a realistic pump pulse curve that generalizes the experimental data presented in Fig. 1, *a*. The dotted curve simulates the behavior of the threshold current under the assumption that the thermal operation mode of the active region is of the adiabatic character, i.e. without energy exchange with the environment. The region where the pump current exceeds the threshold value, i.e. time moments when the laser is capable of emitting, is shaded. Based on the shape of this region, the following conclusions may be made. First, the presence of a maximum in the radiation signal time sweep is due to the threshold current linearly increasing with time, which is valid in the adiabatic approximation at a constant pumping power. Second, beginning from a certain time point, the steady-state pump current becomes insufficient to overcome the threshold, which shall lead to the lasing turn-off.

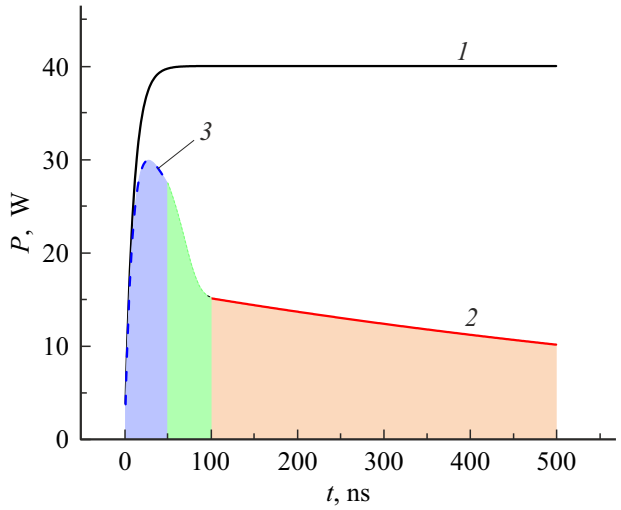

Figure 3. Time sweep of the total power consumption (black line *1*) and its portion spent on heating the active region, which was calculated as a result of processing the experimentally measured rate of radiation power degradation (red line *2*) and in the framework of the model of small heat leakage from the adiabatically heated active region (blue line *3*). The green area illustrates the transient process between the mentioned modes. The color shading shows the area under the curve which will be further used to estimate the laser chip temperature. The colored figure is given in the electronic version of the paper.

Comparison of the presented theoretical calculations with experimental measurements reveals significant differences in them (Fig. 2, *b*). By the end of a 500 ns pulse, the QCL emission decreases by about a third, which evidences that adiabatic approximation provides a significant overestimation of the emission intensity decrease. The results of processing the watt-ampere characteristics presented in Fig. 1, *b* show that, regardless of steepness of the pump pulse front edge, differential efficiency (the watt-ampere characteristic slope) is equal to $k = 0.6$ W/A. Then, assuming that threshold current is a function of time and conditions ensuring lasing are met, obtain that radiation intensity is $A(t) = k\big(I_p(t) - I_{thr}(t)\big)$, where I_p is the pump current. This means that, after the pump current reaches its equilibrium value, time derivative of the measured radiation intensity characterizes only the rate of threshold current variation:

$$I'_{thr}(t) = -k^{-1}A'(t). \tag{2}$$

Estimation of experimental data on the laser radiation time sweep shows that the QCL signal under steady-state pumping is well approximatable by exponential function $A(t) = P_A \exp(-t/\tau_A)$, where $P_A = 0.65$ W, and $\tau_A = 1\,\mu$s. This means that the rate of the radiation intensity reduction obeys the following relation: $A'(t) = -\frac{P_A}{\tau_A}\exp(-t/\tau_A)$. Thus, in 100 and 450 ns after the onset of a pulse with the equilibrium current $I_0 = 4.5$ A, the rate of the signal reduction is -0.6 and -0.4 mW/ns, respectively. Being substituted into formula (2) which relates temporal variations in the threshold current and radiation intensity, these values provide the estimates of the threshold current variation rate of about 1 and 0.7 mA/ns at the pulse onset and end, respectively.

In the adiabatic approximation, the threshold current variation is described by (1) where T_0 is the temperature constant of the threshold current variation measured for the sample under study by the direct method and being equal to 125 K [13]. In this case, if the pump pulse front edge rises infinitely fast, the temperature variation rate is

$$T_{adiab}(t) = \frac{UI_0 t}{C_{AR}}, \tag{3}$$

where $C_{AR} = c\rho V$ is the heat capacity of the active region, I_0 is the pump current stationary value. Substituting here the actual values of current, voltage, characteristic active region volume, and mean values of density and heat capacity for the active region semiconductor compound [14,15], obtain characteristic value $T_{adiab}(t) = t \cdot 0.1$ K/ns. Then the rate of threshold current variation is 2.4 mA/ns, which is approximately 2.5 and 4 times higher than the values determined experimentally in 100 and 450 ns after the pulse onset. Based on this, we can conclude that the temperature profile in the active region vicinity ensures removal of the most part of power consumed by the device in 100 ns.

Fig. 3 summarizes the obtained results. Curve *1* represents the total power consumption for the case of a realistic steepness of the pump pulse front edge and specified pulse parameters. Curve *2* represents power $P_{heating}$ spent on heating the active region, which was obtained by processing experimental data on the pulse $A(t)$ shape, in the following form:

$$P_{heating} = \frac{dQ_{heating}}{dt} = C_{AR}\frac{dT}{dt} = C_{AR}\frac{T_0}{I_{thr}}I'_{thr}(t)$$
$$= -C_{AR}\frac{T_0}{I_{thr}}\frac{A'(t)}{k}, \tag{4}$$

Substituting here $A'(t)$, obtain

$$P_{heating}(t) = \frac{C_{AR}T_0P_A}{I_{thr}k\tau_A}e^{-\frac{t}{\tau_A}}. \tag{5}$$

One can see that the temperature balance established during hundreds of nanoseconds provides wrong estimation of the processes occurring at the moment of the pump pulse onset if curve *2* in Fig. 3 is extrapolated to the region of several nanoseconds, since in this case the power spent on heating the active area will exceed the total power.

To explain this disagreement, consider the following model. Let the energy released at the very beginning of the pump pulse provide uniform heating of the active region according to the adiabatic law. Let the energy leaving the active region be insignificant and distributed over the plate thickness so that its temperature obeys exponential law $T(t, z) = T_{adiab}(t)\exp\big(-\frac{z}{2\sqrt{\alpha t}}\big)$, where α is the thermal diffusion coefficient [cm^2/s], z is the coordinate directed

along the structure growth inside the plate, t is the time since the start of pumping. In this case, heat leakage from the active region bulk is determined by the temperature gradient at its interface with the plate material:

$$P_{leakage}(t) = -\kappa S \frac{\partial T}{\partial z}(t, z = 0), \quad (6)$$

where κ is the plate heat conductivity coefficient, S is the laser area. As long as the leakage is small, partial contribution of the power consumption to the active region heating may be defined in the approximation of the realistic pump pulse front as

$$P_{leakage}(t) = \kappa S \frac{U \int_0^t I_p(x)dx}{C_{AR}} \frac{1}{2\sqrt{\alpha t}}. \quad (7)$$

In this case, the power spent on heating the active region is $P_{heating}(t) = P_{total}(t) - P_{leakage}(t)$. Fig. 3 presents the curve of this function in the interval of 0–50 ns (line *3*). Apparently, in the 0–30 ns region this curve is close to the adiabatic approximation. The indicated limit of 30 ns relates to the moment when the phonon diffusion in the plate is characterized by spatial constant $2\sqrt{\alpha t} \approx 2\,\mu$m (for InP) which is comparable with the active region and plate thicknesses equal to 2 and 4 μm, respectively. This may be interpreted as follows: during the first 50 ns from the moment the pulse is applied, most of the released thermal energy is spent almost adiabatically on heating the active region, but a certain portion of it diffuses into the plates thus creating a primary heat leakage channel. In the 50–100 ns interval, the temperature gradient in the plate gets equalized, which makes the temperature an almost linear function of the plate thickness. After 100 ns, there opens an overall leakage channel for the thermal energy releasing into the radiator. After 450 ns, the temperature gradient in the plate changes slowly, and its total increase during the transition to the stationary mode is no more than twofold, since already in 450 ns the gradient removes about 75% of the released power.

Thus, in this work we have examined the influence of the active region heating on the QCL operation in the pulsed mode. We have shown that, in the mode with the sub-microsecond pulse duration, the device thermal regime can be assumed to consist of three phases. The first phase (in the interval of 0–50 ns) is characterized by almost adiabatic active region heating and formation of a preliminary (nonlinear) temperature gradient in the plates. The second phase (50–100 ns) is accompanied by further heating of the plates, which gives rise to an almost constant temperature gradient in the vicinity of the active region. In the third phase (100–500 ns), formation of a constant gradient in the plate region gets finished, and overall heat removal into the radiator bulk begins. In this time interval, a small part of the total released power is spent on heating the active region. In this study, there was created a theoretical basis for a systematic approach to developing the design of new, more efficient QCLs.

Funding

The study was supported by the Russian Scientific Foundation, project № 23-29-00930.

Conflict of interests

The authors declare that they have no conflict of interests.

References

[1] R. Kazarinov, R. Suris, Sov. Phys. Semicond., **5** (4), 707 (1971).
[2] J. Faist, F. Capasso, D.L. Sivco, C. Sirtori, A.L. Hutchinson, A.Y. Cho, Science, **264** (5158), 553 (1994). DOI: 10.1126/science.264.5158.553
[3] P.I. Abramov, E.V. Kuznetsov, L.A. Skvortsov, M.I. Skvortsova, J. Appl. Spectrosc., **86** (1), 1 (2019). DOI: 10.1007/s10812-019-00775-8
[4] R.J. Grasso, Proc. SPIE, **9933**, 99330F (2016). DOI: 10.1117/12.2238963
[5] B. Panda, A. Pal, S. Chakraborty, M. Pradhan, Infrared Phys. Technol., **125**, 104261 (2022). DOI: 10.1016/j.infrared.2022.104261
[6] X. Pang, O. Ozolins, L. Zhang, R. Schatz, A. Udalcovs, X. Yu, G. Jacobsen, S. Popov, J. Chen, S. Lourdudoss, Phys. Status Solidi A, **218** (3), 2000407 (2021). DOI: 10.1002/pssa.202000407
[7] A. Evans, S.R. Darvish, S. Slivken, J. Nguyen, Y. Bai, M. Razeghi, Appl. Phys. Lett., **91** (7), 071101 (2007). DOI: 10.1063/1.2770768
[8] F. Wang, S. Slivken, D.H. Wu, M. Razeghi, Opt. Express, **28** (12), 17532 (2020). DOI: 10.1364/OE.394916
[9] E. Cherotchenko, V. Dudelev, D. Mikhailov, G. Savchenko, D. Chistyakov, S. Losev, A. Babichev, A. Gladyshev, I. Novikov, A. Lutetskiy, D. Veselov, S. Slipchenko, D. Denisov, A. Andreev, I. Yarotskaya, K. Podgaetskiy, M. Ladugin, A. Marmalyuk, N. Pikhtin, L. Karachinsky, V. Kuchinskii, A. Egorov, G. Sokolovskii, Nanomaterials, **12** (22), 3971 (2022). DOI: 10.3390/nano12223971
[10] A.V. Babichev, V.V. Dudelev, A.G. Gladyshev, D.A. Mikhailov, A.S. Kurochkin, E.S. Kolodeznyi, V.E. Bougrov, V.N. Nevedomskiy, L.Ya. Karachinsky, I.I. Novikov, D.V. Denisov, A.S. Ionov, S.O. Slipchenko, A.V. Lutetskiy, N.A. Pikhtin, G.S. Sokolovskii, A.Yu. Egorov, Tech. Phys. Lett., **45** (7), 735 (2019). DOI: 10.1134/S1063785019070174.
[11] A.V. Babichev, A.G. Gladyshev, A.V. Filimonov, V.N. Nevedomskii, A.S. Kurochkin, E.S. Kolodeznyi, G.S. Sokolovskii, V.E. Bugrov, L.Ya. Karachinsky, I.I. Novikov, A. Bousseksou, A.Yu. Egorov, Tech. Phys. Lett., **43** (7), 666 (2017). DOI: 10.1134/S1063785017070173.
[12] V.V. Dudelev, D.A. Mikhailov, A.V. Babichev, A.D. Andreev, S.N. Losev, E.A. Kognovitskaya, Yu.K. Bobretsova, S.O. Slipchenko, N.A. Pikhtin, A.G. Gladyshev, D.V. Denisov, I.I. Novikov, L.Ya. Karachinsky, V.I. Kuchinskii, A.Yu. Egorov, G.S. Sokolovskii, Quantum Electron., **50** (2), 141 (2020). DOI: 10.1070/QEL17168.

[13] V.V. Dudelev, E.D. Cherotchenko, I.I. Vrubel, D.A. Mikhailov, D.V. Chistyakov, V.Yu. Mylnikov, S.N. Losev, E.A. Kognovitskaya, A.V. Babichev, A.V. Lutetskiy, S.O. Slipchenko, N.A. Pikhtin, A.V. Abramov, A.G. Gladyshev, K.A. Podgaetskiy, A.Yu. Andreev, I.V. Yarotskaya, M.A. Ladugin, A.A. Marmalyuk, I.I. Novikov, V.I. Kuchinskii, L.Ya. Karachinsky, A.Yu. Egorov, G.S. Sokolovskii, Phys. Usp., **67** (1) (2024). DOI: 10.3367/UFNe.2023.05.039543.
[14] S. Adachi, *Physical properties of III–V semiconductor* (John Wiley & Sons, 1992).
[15] H.Y. Lee, J.S. Yu, Appl. Phys. B, **106** (3), 619 (2012). DOI: 10.1007/s00340-011-4744-4.

Translated by EgoTranslating